

## A New Design and Optimization of Capacitive MEMS Accelerometer

M. Sarvghad Moghadam <sup>a,\*</sup>, H. Arefi <sup>b</sup>, Kh. Mafinezhad <sup>a,c</sup>

<sup>a</sup>Sadjad institute of higher education, Emamat Avenue, Mashhad 9188148848, Iran <sup>b</sup>Malek

Ashtar University of Technology, Lavizan Avenue, Tehran 158751774, Iran <sup>c</sup>Ferdowsi  
University, Azadi Avenue, Mashhad 9177948974, Iran

\* Corresponding author: m.sarvghadmoghadam@yahoo.com

**Abstract** - In this paper, design and optimization of a folded beam for a shunt capacitive MEMS accelerometer is presented together with a comparison of important parameters to five beams with different geometries in range of 20g -100g for crash detection. The structure contains a proof mass which is suspended over fixed rigid pull-down electrode to provide capacitance measurement. Powerful soft wares (COVENTOR, ANSYS and MATLAB) are used for finite element analysis (FEA) modeling and simulation. In order to have a good comparison, nonlinear dynamic models such as elastic deformation, residual stress, and squeeze film damping, Q-factor, stiffness coefficient, resonant frequency, electrostatic in addition to some other important parameters on mechanical performance have been studied. The results obtained from both the analytical and finite element models proved to be desirable.

**Keywords** — MEMS, Accelerometer, Critical collapse voltage, Electrostatic, Fixed-Fixed beam

### I. INTRODUCTION

The extraordinary combination of advantages associated with micro-electromechanical systems (MEMS) like small size, low cost, multifunction, low power consumption, and easy integration with consumer electronics has been the primary design issue for commercial micro-electromechanical system (MEMS) applications such as inertia sensors and microphones [1].

Effort has been made toward making smaller and more precise MEMS sensors. In particular, MEMS accelerometers became a core part of many engineering systems, starting from consumer electronics, such as digital cameras, cellular phones, computer games, and airbag systems, and up to high-end devices for sophisticated navigation and guiding systems for defense applications [2]. The fields of MEMS accelerometers have been used as crash sensors in automotive airbag systems for more than ten years [3].

The MEMS accelerometers usually consist of a proof mass suspended using an elastic element (spring). When the device is accelerated, an inertial force is applied to the proof mass, resulting in its deflection in the direction opposite to the applied acceleration [2]. The acceleration can be extracted from the measuring of the capacitance between suspension element and electrode stress in the suspension elements.

In many MEMS applications, capacitive detection is known to offer several benefits compared to other sensing methods, especially due their ease of implementation. Capacitive methods do not require integration of a special material, which makes them compatible with almost any fabrication process. They also provide good DC response and noise performance, high sensitivity, low drift, and low

temperature sensitivity [4]. Therefore, in this paper, a folded beam is designed to be implemented in capacitive accelerometers applied in airbags.

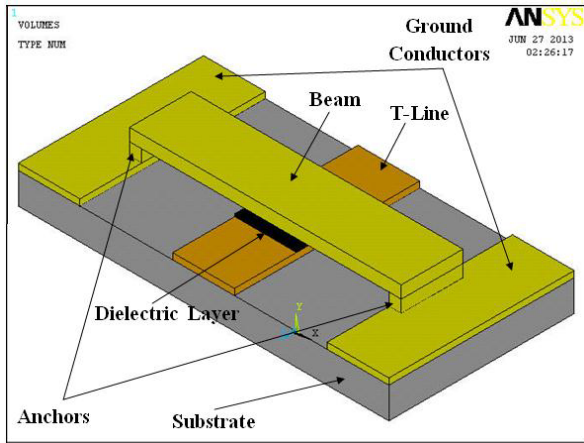
Beam stiffness is one of the most important parameters which have been studied in field of MEMS devices. Stiffness plays an important role in decreasing critical collapse voltage of capacitive accelerometers. It shall be considered, however, that decreasing stiffness causes low security of capacitive MEMS devices. Therefore, good optimization should be done for these two parameters. Other parameters such as resonance frequency, sensitivity, Q-factor, mass, size and also mechanical properties should be considered in design. In this paper, design and optimization of a kind of folded beam for automotive airbag system is studied and compared to five beams with different geometries.

This paper is organized as follows: section II describes basic accelerometer structure and gives in detail the operational principle. Section III presents a brief analysis of electrostatic actuation followed by section IV which relates the discussion to dynamic behavior of the device. Section V concludes the papers.

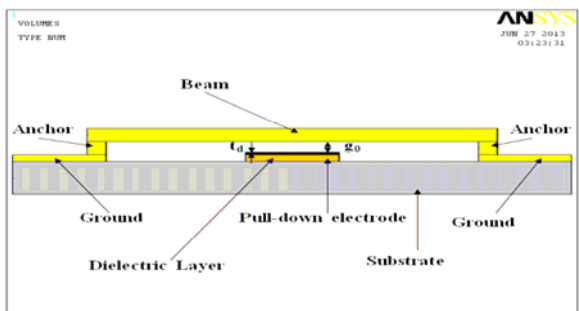
### II. ACCELEROMETER STRUCTURE

Fig.1 Shows schematic view of a shunt capacitive MEMS accelerometer. The device includes a thin gold metal membrane which is called "beam". This beam, which is given with a simple design for better understanding, is suspended over a thin silicon nitride dielectric layer deposited on the upper surface of a transmission line (T-line). Both ends of the beam are connected to ground conductors through anchors. When a voltage is applied between this fixed-fixed beam and the

pull-down electrode, an electrostatic force is induced on the beam and pulls it down toward the dielectric layer. The dielectric prevents direct contact between the beam and the pull-down electrode.



(a)



(b)

Fig.1. Schematic of a shunt capacitive MEMS accelerometer a) top view b) cross section view

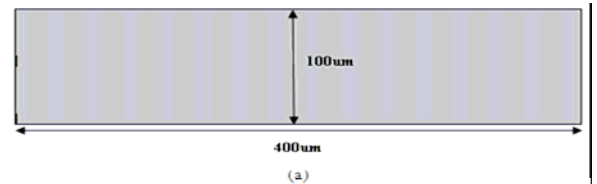
**A. Typical geometries for beam structures**

Thus far a great number of geometries have been introduced to optimize the beam performance. Fig. 2 shows some common geometries for beam structures used in shunt capacitive MEMS accelerometers [5,6]. The spring stiffness of these beam structures decrease respectively from (a) to (d) in Fig.2, and their values are given later in another section.

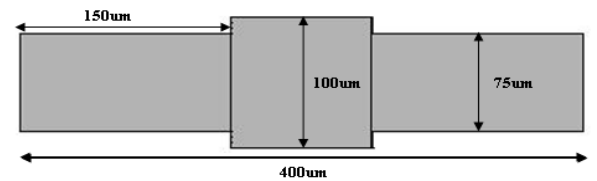
**B. Proposed beam structure**

The schematic view of the proposed folded beam presented in this paper is illustrated in Fig.3. The device is made up of springs that are fixed to the ground by 4 anchors. The main advantage of this beam is that while maintaining the same good mechanical and elasticity properties presented in Fig.3, it enjoys a significantly

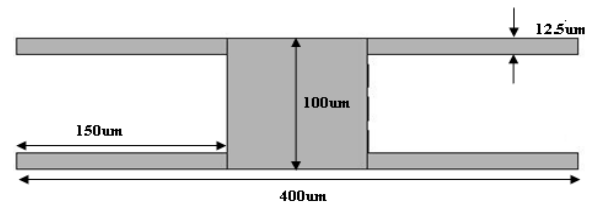
more compact size. Fig.3 shows top view of the proposed beam with  $L = 140$  micrometers in length also  $w = 5$  and  $t = 3$  micrometers that respectively are width and thickness of the proposed beam.



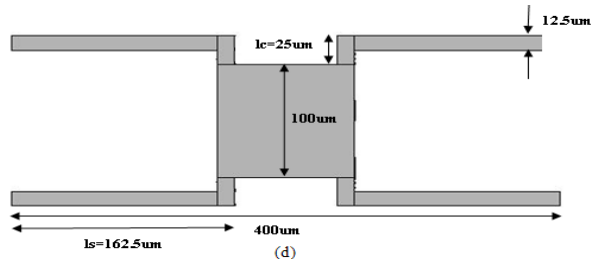
(a)



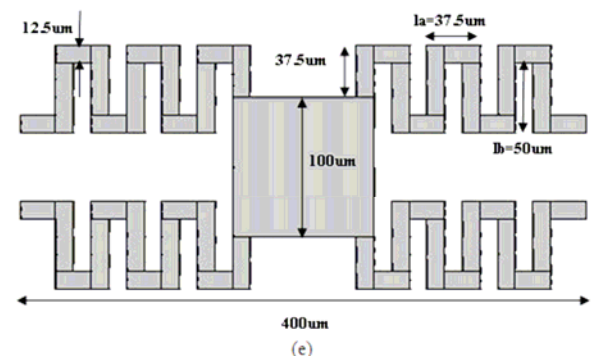
(b)



(c)



(d)



(e)

Fig.2. Typical geometries for beam structures a) Structure 1 b) Structure 2 c) Structure 3 d) Structure 4 e) Structure 5

The pull-down electrode, located under the beam, is 100 micrometers in width ( $W$ ). The gap  $g$  between the beam and the dielectric layer is equal to 2 micrometers. The advantages achieved by this scheme are low actuation voltage, high sensitivity, high speed, low cost, low noise,

low power consumption and with an optimal quality factor.

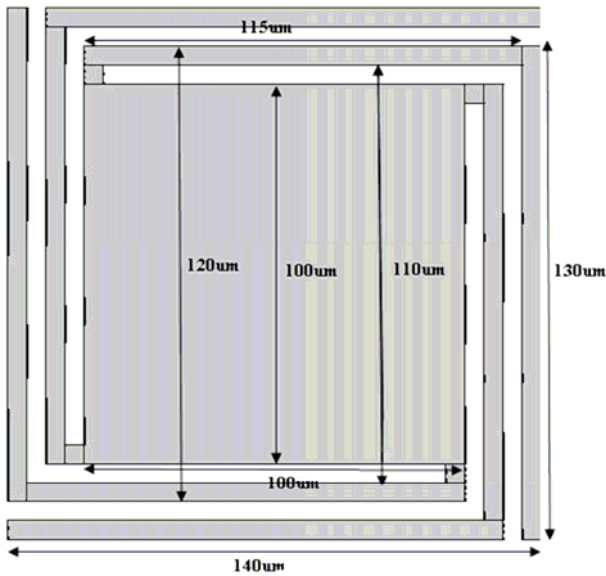


Fig.3.Schematic top view of proposed beam

The mechanical parameters of the proposed and conventional beams are presented in Table I.

TABLE I. MATERIAL AND GEOMETRIC PARAMETERS

Symbol	Quantity	value
L	Length of the beam	400 μm
w	Width of the beam	100 μm
L <sub>2</sub>	Pull-down electrode length	100 μm
t	Thickness of the beam	3 μm
ε <sub>0</sub>	Permittivity of air	8.854 × 10 <sup>-12</sup> F/m
ε <sub>r</sub>	Relative Permittivity of dielectric layer	7.6
E <sub>Au</sub>	Young's modulus	80 GPa
ρ <sub>Au</sub>	Specific mass of material	19320Kg/m <sup>3</sup>
ν <sub>Au</sub>	Poisson's ratio of Au	0.41
g <sub>0</sub>	Initial gap	2 μm
t <sub>d</sub>	Thickness of the dielectric layer	0.2 μm

C. Effective Stiffness Coefficient

Beams stiffness coefficient used in capacitive accelerometers is one of the important characteristics that play an important role in the dynamic and frequency analysis. When the beam bends the gap between it and pull-down electrode changes. The effective stiffness coefficient of the fix to fix beam is given by [6].

$$K = 10Ew\left(\frac{t}{l}\right)^3 \tag{1}$$

where F is the electrostatic force over the center of structure, and δ max the maximum deflection. Equation (3) presents the effective stiffness coefficient for the proposed beam, which is calculated using equations 1 and 2.

$$\delta_{\max} = \frac{Fl^3}{120EI} \tag{2}$$

This results in:

$$K = 10Ew\left(\frac{t}{l}\right)^3 \tag{3}$$

where E is Young's modulus, I is moment of inertia, w width of the beam, t thickness of the beam, l length of the beam and δ max is the maximum deflection. Table II shows the values of effective stiffness coefficient for conventional and proposed beam.

TABLE II. EFFECTIVE STIFFNESS FOR CONVENTIONAL AND PROPOSED BEAM

Stiffness coefficient (K)	Value ( $\frac{N}{m}$ )
Structure 1	108
Structure 2	96
Structure 3	32
Structure 4	24.5
Structure 5	7.77
proposed Beam	6.9

III. ELECTROSTATIC ACTUATION

As pointed out before, when a voltage is applied between a beam and the pull-down electrode, an electrostatic force is induced on the beam deflecting it down toward the dielectric layer, which leads to a change in capacitance. By this change, the correspondent acceleration is measurable.

As an approximate model, the combination of the beam over the pull-down electrode can be modelled as a parallel-plate capacitor. Any change in the gap size between the parallel plates would cause a change in the capacitance value which leads to measurement of acceleration. The applied voltage, called actuation voltage, is dependent on factors like geometry, material properties, dielectric layer thickness and gap between the beam and dielectric layer. Equating the applied electrostatic force with mechanical spring force results in equation (4). Solving this equation for actuation voltage V, equation (5) is found [5,7].

$$\frac{1}{2} \frac{\epsilon_0 w W V^2}{g^2} = K(g_0 - g) \tag{4}$$

$$V = \sqrt{\frac{2Kg^2(g_0 - g)}{\epsilon_0 w L^2}} \tag{5}$$

The actuation voltage cannot exceed a limited value because of possible instability which leads to collapse of the beam. We should note that the maximum displacement of the beam must be  $g_0/3$ .

We can find the critical collapse voltage from [5,7]:

$$V = \sqrt{\frac{8 K_{eff} g_0^3}{27 \epsilon_0 w L^2}} \quad g = \frac{2}{3} g_0 \tag{6}$$

The reduction of actuation voltage for capacitive accelerometers is an advantage, which is lower in the proposed beam as to other beams in [5,6]. The gap size is related to the critical collapse voltage value. This is plotted in Fig.4 for the proposed beam using COVENTOR Ware.

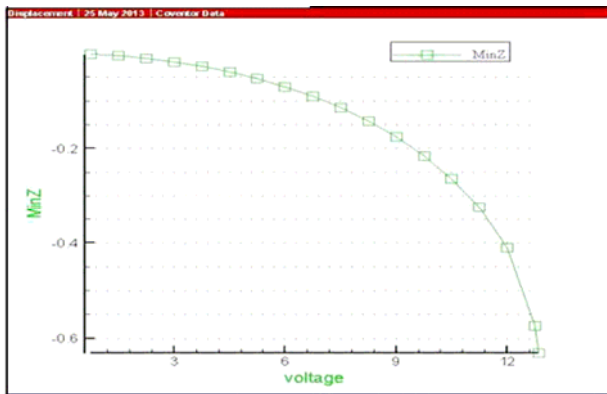


Fig.4. The relation of gap and actuation voltage for pull-in instability concept for the proposed beam

A calculation-based comparison between actuation voltages of the conventional and the proposed beams is shown in Fig.5.

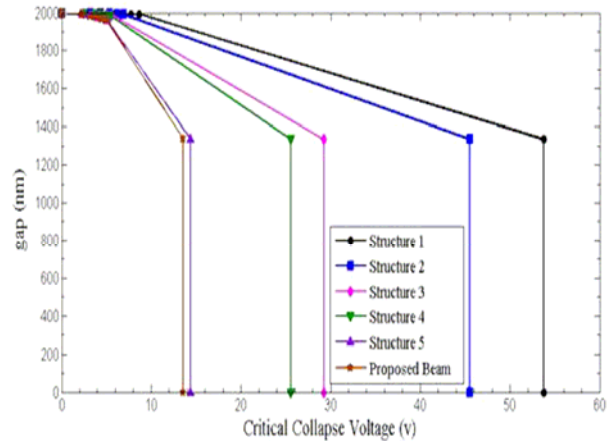


Fig.5. The relation of gap and actuation voltage for pull-in instability concept for the conventional and proposed beams

Table III is the numerical representation of Fig 5.

TABLE III. CRITICAL COLLAPSE VOLTAGES BASED ON CALCULATION AND SIMULATION

Types of the beam	Calculated value	Simulated value
Structure 1	53.77	53
Structure 2	45.56	45
Structure 3	29.27	29
Structure 4	25.61	25
Structure 5	14.42	14
proposed Beam	13.6	13

#### IV. DYNAMIC BEHAVIOR

##### A. Resonant frequency and displacement sensitivity

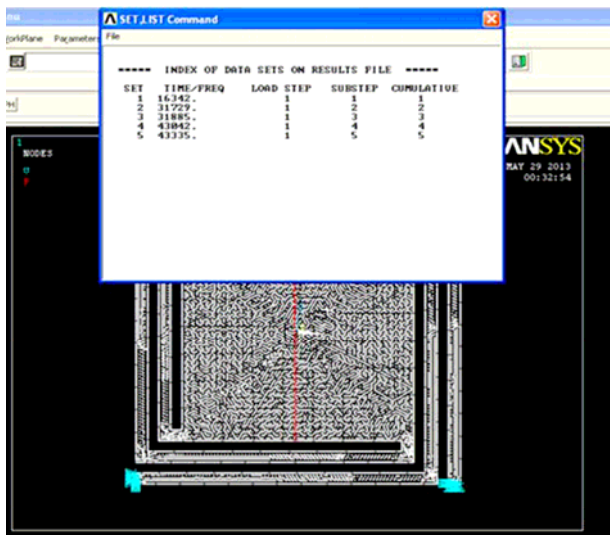
Generally, for MEMS devices to design, structural and vibration analysis is the starting point. Therefore, stiffness constant and resonant frequencies are two important parameters of much priority. Stiffness constant, which is a crucial factor in determining the resonant frequency and sensitivity, is obtained through a combination of the geometric parameters and physical properties of the material. However, resonant frequency determines bandwidth and physical sensitivity of the accelerometer. Accelerometer displacement sensitivity and resonant frequency of the following relations are obtained by [8,9].

$$f_r = \frac{1}{2\pi} \sqrt{\frac{K}{m_s}} \quad (7)$$

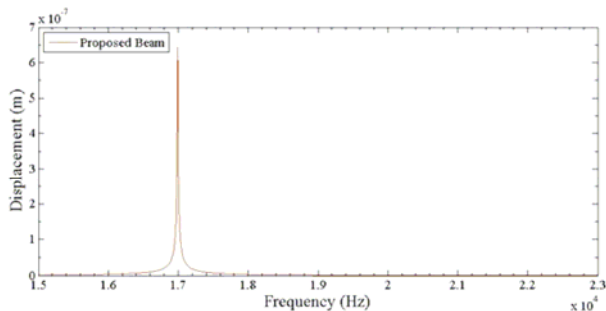
$$S_d = \frac{\delta_{max}}{a} \quad (8)$$

where  $f_r$  is the resonant frequency,  $K$  the effective stiffness coefficient,  $m_s$  the total proof-mass and effective mass of the springs,  $S_d$  the displacement sensitivity,  $\delta_{max}$  the maximum deflection, and  $a$  is the acceleration.

In Fig.6, five first mode resonant frequencies obtained from the proposed beam is presented. In addition, the first order resonant frequency of the proposed beam is simulated using MATLAB, which shows good agreement with the same results obtained from ANSYS shown in Table IV.



(a)



(b)

Fig.6. Simulated resonant frequency of the proposed beam a) by ANSYS b) by MATLAB.

It should be noted that the sensitivity is inversely related to resonant frequency. As seen, the sensitivity of the proposed beam is higher.

TABLE IV. SIMULATED VALUES OF THE RESONANT FREQUENCY BEAMS OF THE FIRST TO FIFTH ORDER.

The first order resonant frequency ( $f_r$ )	ANSYS	MATLAB	$S_d$ (nm/g)
Structure 1	54.938	58.060	0.078
Structure 2	50.741	51.510	0.083
Structure 3	34.600	36.830	0.111
Structure 4	30.574	32.060	0.139
Structure 5	20.501	18.440	0.385
proposed Beam	16.342	16.990	0.421

*B. Damping coefficient, Damping Ratio, Quality Factor*

The presence of gas in the oscillating structure and its stickiness effect, determines the Damping associated with the structure. The stickiness damping effect can be modeled using the general squeeze film damping coefficient. Equation (9) is a simplified form of Reynold’s equation and is commonly used to obtain the coefficient damping for oscillatory structures [10].

$$B = \frac{\mu l w^3}{g^3} \beta(\eta) \quad (9)$$

where  $g$  is the gap,  $w$  the width,  $l$  the length of the beam,  $\eta$  the gas viscosity equal to  $w / L$ ,  $\beta(\eta)$  is a correction factor related to the ratio of width to length is indicated in Fig.7 [10].

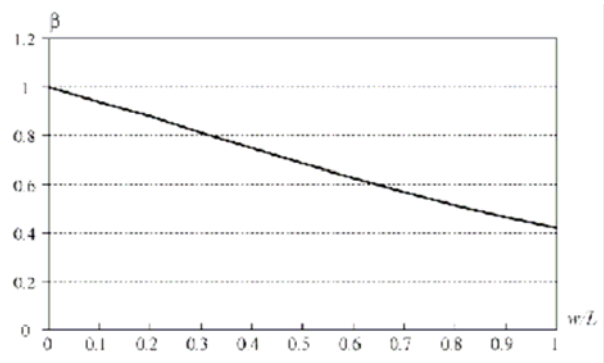


Fig.7. The dependence of the coefficient factor of width to length  $w / L$ ,  $\beta(0) = 1$ ,  $\beta(1) = 0.42$  and  $(w = L)$  [10].

For the sensor to be stable at resonant frequency resulting in better sensitivity, the damping has been calculated in vacuum pressure. The quality factor  $Q$  of the beam is given in (11) using the damping rate  $\zeta$  in (10) is found [8].

$$\zeta = \frac{b}{2\sqrt{mK}} = \frac{b}{2mK} \quad (10)$$

$$Q = \frac{\omega_n}{\omega_2 - \omega_1} = \frac{1}{\sqrt{1+2\zeta} - \sqrt{1-2\zeta}} \quad (11)$$

Using COVENTOR Ware, the variation of damping coefficient for the proposed beam at different frequencies is simulated, as is shown in Fig.8. Besides, as presented in Table V, three important factors for several types of beams have been obtained by calculation.

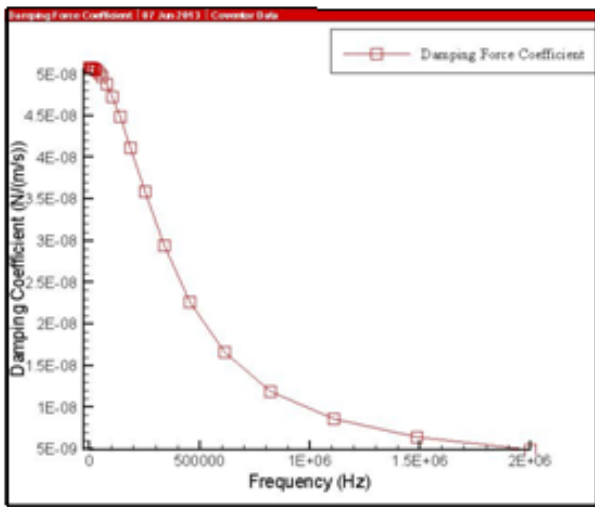


Fig.8. Simulation result for the damping coefficient variation with frequency

Besides, as presented in Table V, three important factors for several types of beams have been obtained by calculation.

TABLE V. DAMPING COEFFICIENT, Q-FACTOR AND DAMPING RATIO OF DIFFERENT TYPES OF THE BEAMS INCLUDING THE PROPOSED BEAM

Types of the beam	Damping Coefficient(N.s/m)	Q-Factor	Damping ratio
Structure 1	$7.6 \times 10^{-8}$	3906	$128 \times 10^{-6}$
Structure 2	$7 \times 10^{-8}$	3226	$155 \times 10^{-6}$
Structure 3	$5.1 \times 10^{-8}$	2092	$239 \times 10^{-6}$
Structure 4	$5.1 \times 10^{-8}$	1894	$264 \times 10^{-6}$
Structure 5	$5.2 \times 10^{-8}$	1362	$367 \times 10^{-6}$
proposed Beam	$5.1 \times 10^{-8}$	900	$556 \times 10^{-6}$

### C. Variable capacitance and FOM

#### C.1. Variable capacitance

When the beam is at the actuated state, the dielectric between two contacts exhibits a varied capacitance, given by [5].

$$C = \frac{\epsilon_0 A}{g + \frac{t_d}{\epsilon_r}} \quad (12)$$

where  $A = wL_2$ , is the overlap area between the pull-down electrode and the beam.

#### C.2. Figure of merit (FOM)

The figure of merit (FOM) is the ratio of the capacitance, when the beam is in the down-state mode, over the capacitance when it is in up-state mode, as given by [5]:

$$FOM = \frac{C_d}{C_u} = \frac{\frac{\epsilon_0 \epsilon_r A}{t_d}}{\frac{\epsilon_0 A}{g_0 + \frac{t_d}{\epsilon_r}}} \quad (13)$$

where the notations have already been presented in Table I. Larger values for this figure of merit would be closer to the ideal condition.

Keeping equal the figures of merit of all the different types of beams, including the proposed one, we tried to improve several other parameters in the proposed beam. The equalized value of FOM for all the beams is 77.

#### D. Comparison between different parameters of the Conventional and proposed beams

To make an accurate assessment of the conventional and proposed beams used in capacitive accelerometer a number of important parameters like stress, deflection, actuation voltage in range 20g to 100g for crash detection in automotive which are simulated [11]. Fig.9 shows a simulated-base comparison between maximum deflection versus acceleration of the conventional and proposed fixed-fixed beams. As seen, the deflection under the applied acceleration is the highest in the proposed beam.

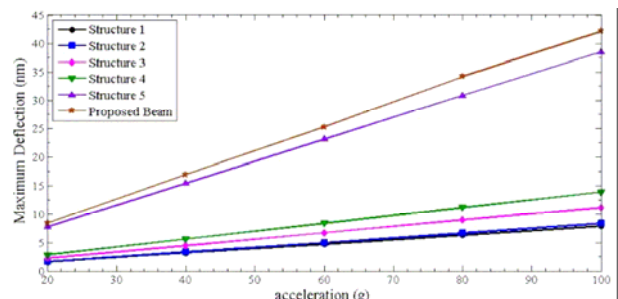


Fig.9. Maximum deflection vs. the acceleration for conventional and proposed fixed-fixed beams

One of the advantages of the proposed beam is the

reduced actuation voltage proportional to other beam, as clearly demonstrated in Fig.10.

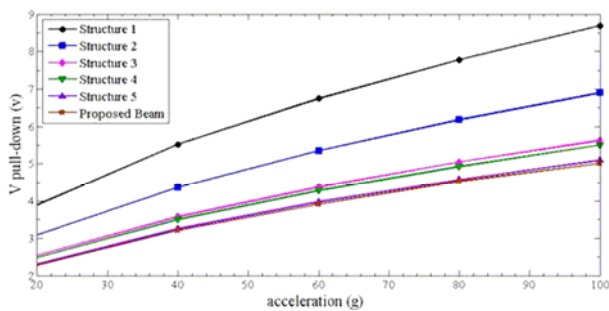


Fig.10. Pull-down voltage vs. the acceleration for conventional and proposed fixed-fixed beams

Moreover, Fig.11 shows the simulated results for capacitance in the specified range of different acceleration values for conventional and proposed fixed-fixed beams.

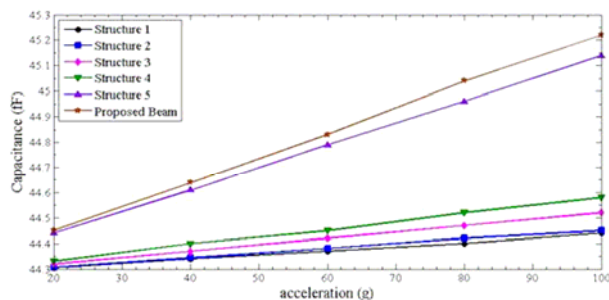


Fig.11. Capacitance vs. the acceleration for conventional and proposed fixed-fixed beams

Finally, simulation results of the maximum stress for acceleration equal to 20g of the conventional and proposed fixed-fixed beams are shown in Fig.12.

### E. Modified proposed beam

The main disadvantage of this design is that after applying acceleration, the four joining parts where the springs connect to the proofmass experience the maximum amount of stress.

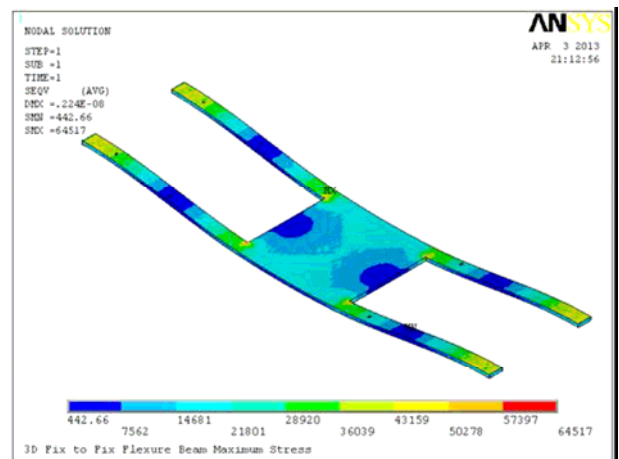
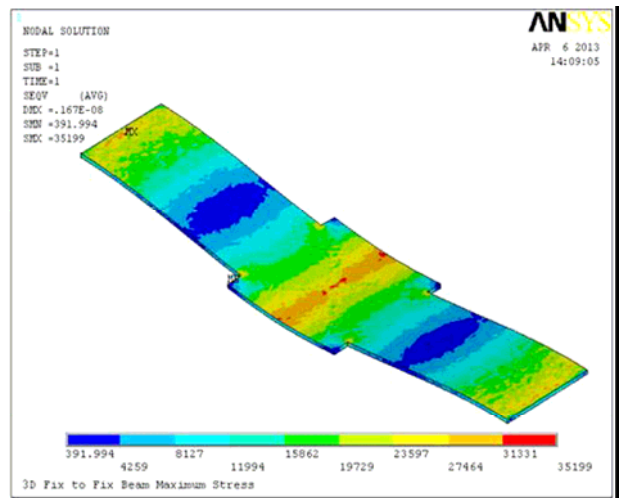
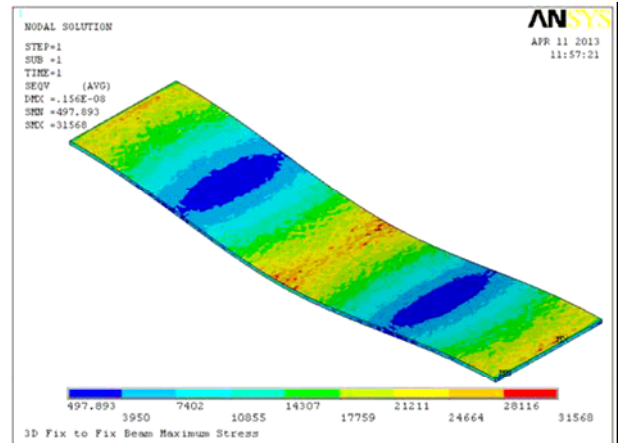


Fig.12-A. Simulation results of the maximum stress for an acceleration equal to 20g of the conventional and proposed fixed-fixed beams

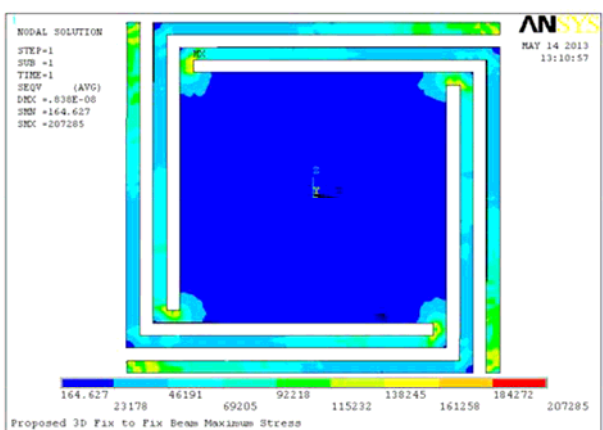
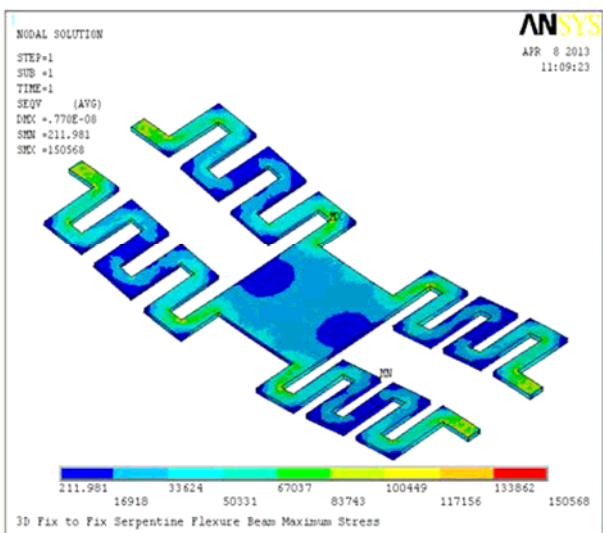
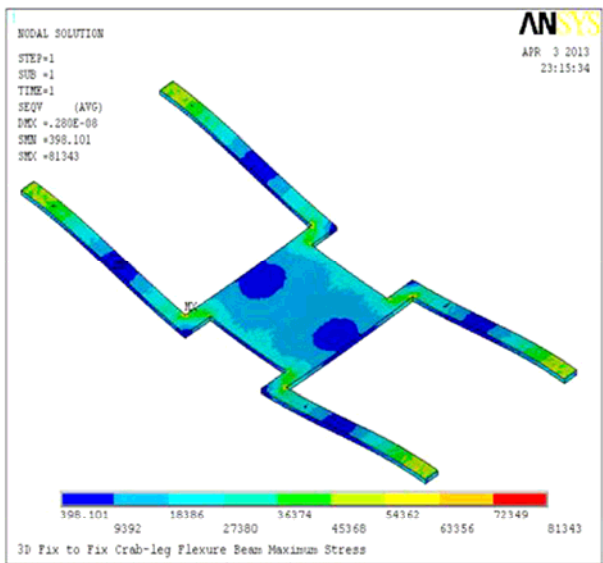


Fig.12-B. Simulation results of the maximum stress for an acceleration equal to 20g of the conventional and proposed fixed-fixed beams.

To improve this drawback, the inner side of the joining parts were modified from a straight-line form into a curved arc shape, which leads to the reduction of the maximum stress by 4MPa. Fig.13 shows the schematic top view of the modified proposed beam.

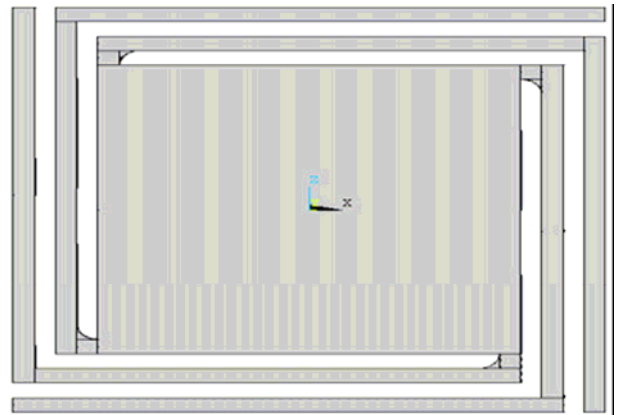


Fig.13. Schematic top view of the modified proposed beam

The simulated illustration of the maximum stress induced on the modified proposed beam is shown in Fig.14.

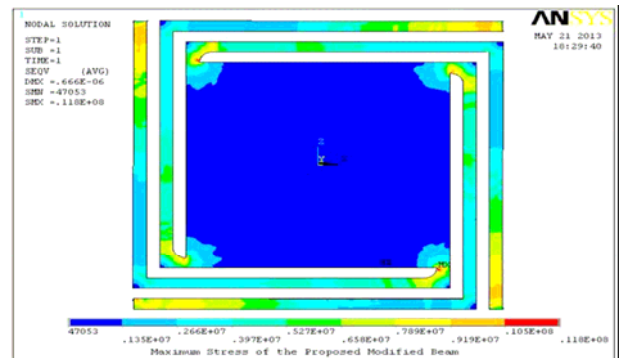


Fig.14. Schematic top view of the modified proposed beam

The comparative results of the simulated residual stress for different beams, including the modified proposed beam, are given in Fig15. It is clear from this figure that residual stress in the proposed beam assumes higher quantities than others as is shown in Fig15. The modified proposed beam presents quite a sensible decrease in the above mentioned parameters making its graph take a place much closer to that of other beams.

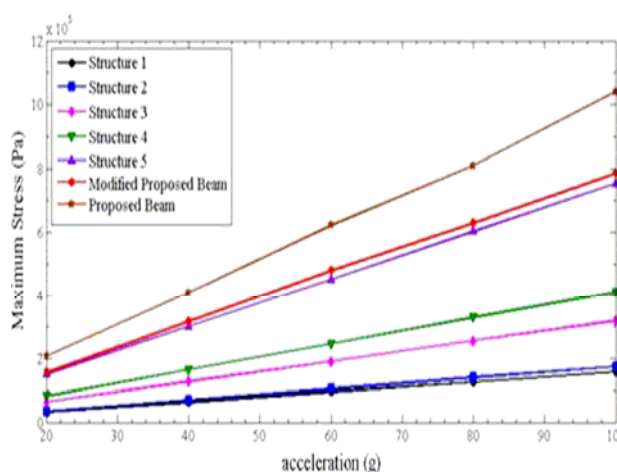


Fig.15. Maximum stress vs. the acceleration for conventional and proposed fixed-fixed beams

## V. CONCLUSION

A comparative study is made for the analytical and FEA results of five beams with different geometries to apply in capacitive accelerometer. Then a new design of folded beam which has better mechanical and dynamic properties is presented.

COVENTOR and ANSYS softwares are used to model simulate and carry out FEA analysis. An analytical model is also simulated using MATLAB and the results obtained by FEA are in close agreement with the analytical results.

One of the important aspects in the capacitive micro machined accelerometers is the dynamic response. The dynamic response can be estimated from the equivalent spring-mass model which predicts resonance frequency and electrostatic analysis.

Design and optimization of folded beam for airbags system in range of 20g-100g is studied and compared to five beams with different geometries. Smaller size (almost 1/3 other presented beam sizes) and lower mass of designed folded beam could establish small MEMS sensors. Decreasing in actuation voltage and making critical collapse voltage of folded beam lower, which is reported in current paper (almost 13.6 volts), represents better optimization than other five beams leading to proper power consumption sensors, higher sensitivity and appropriate Q-factor with acceptable mechanical features and making the proposed folded beam a good choice for MEMS inertial sensors such as accelerometers.

## REFERENCES

- [1] Chih-Ming Sun, Ming-Han Tsai, Yu-Chia Liu, and Weileun Fang, Member IEEE, "Implementation of a Monolithic Single Proof-Mass Tri-Axis Accelerometer Using CMOS-MEMS Technique," IEEE TRANSACTIONS ON ELECTRON DEVICES, VOL. 57, NO. 7, JULY 2010.
- [2] Assaf Ya'akovovitz and Slava Krylov, "Toward Sensitivity Enhancement of MEMS Accelerometers Using Mechanical Amplification Mechanism," IEEE SENSORS JOURNAL, VOL. 10, NO. 8, AUGUST 2010.
- [3] Jian Wen, Vijay Sarihan, Bill Myers, and Gary Li, "A Multidisciplinary Approach for Effective Packaging of MEMS Accelerometer," 2010 Electronic Components and Technology Conference IEEE.
- [4] Cank Acar and Andrei Shkel, "MEMS VIBRATORY GYROSCOPES," Springer 111-112, June 2008.
- [5] G. Rebeiz, RF MEMS Theory, Design and Technology, New Jersey, J. Wiley, & Sons, 2003.
- [6] J.-M Huang, K.M. Liew, C.H. Wong, S. Rajendran, M.J. Tan, A.Q. Liu, "Mechanical design and optimization of capacitive micro-machined switch," 2001 Elsevier Science, Sensors and Actuator A 93 (2001) 273-285.
- [7] Divya Verma, Ajay Kaushik, "Design And Performance Analysis of Meander Structure RF-MEMS Capacitive Switch" International Journal of Engineering Research and Applications Vol. 2, Issue 2, Mar-Apr 2012, pp.595-598.
- [8] James J. Allen microelectromechanical system Design, Taylor & Francis Group, LLC pp 102-103, 2005.
- [9] Stephen Beeby ,Graham Ensell,Michael Kraft and Neil White, MEMS Mechanical Sensors, ARTECH HOUSE pp 119-120 , INC ,2004.
- [10] Minhang Bao, Heng Yang, "Squeeze film air damping in MEMS," Science Direct Trans. M. Bao, H. Yang, Sensors and Actuators a 136 (2007) 3-27.
- [11] Dr. j. marek, H. P. Trah, Y. Suzuki, I. Yokomori, "Sensors for automotive technology," WILEY-VCH (2003).

## Biographies

**M. Sarvghad Moghadam** was born in Mashhad, Iran on September 21, 1986. He received the Bachelor's degree in communications engineering, and the master's degree in electronics engineering from Sadjad Institute of Higher Education, Mashhad, Iran in 2010 and 2013 respectively. He is with Sadjad Institute of Higher Education Research Center. His main research interests include the development and application of micro-electromechanical-systems (MEMS) technology and devices, with a focus on complementary inertial sensors, as well as electrostatic actuators, and design of automotive MEMS accelerometers.

**Hamed Arefi** received the Bachelor's degree in electrical engineering from Sadjad Institute of Higher Education, Mashhad, in 2010, the master's degree in electrical engineering from Malek Ashtar Industrial University, Tehran, in 2013 respectively. He is with Laboratory of Micro fabrication at Malek Ashtar Industrial University, where his research is focused on inertial MEMS sensors. Malek Ashtar Laboratory is one of the best laboratories in the field of micro fabrication in Iran. His research

interests include inertial magnetic and accelerometer MEMS sensors.

**Kh. Mafinezhad** was born in Mashhad, Iran in 1947. He received his BS degree in communication engineering from Khagenassir University, Tehran, Iran in 1972, and the MS and PhD degrees in high frequency electronic from the "Ecol National Superieur De Telecommunication de Paris, France in 1978 and 1981 respectively. From 1981 till now he was assistant and then associate professor of Engineering Faculty of Ferdowsi University, Mashhad, Iran. He was the director of research center of Sadjad Higher Education Institution from 1998 to 2008. He has been an editorial board member of IAEEE journal since 2004 and journal of Azad Mashhad University since 2006. He was chairman of 12th Iranian Conference on Electrical Engineering (ICEE) in Ferdowsi University. He is the author or coauthor of more than 100 papers and articles published in international conferences and scientific journals. His research interest includes high frequency circuits, nonlinear modeling and RFMEMS.